



SAR thresholds for electromagnetic exposure using functional thermal dose limits

Fatemeh Adibzadeh, Margarethus M. Paulides & Gerard C. van Rhoon

To cite this article: Fatemeh Adibzadeh, Margarethus M. Paulides & Gerard C. van Rhoon (2018) SAR thresholds for electromagnetic exposure using functional thermal dose limits, International Journal of Hyperthermia, 34:8, 1248-1254, DOI: [10.1080/02656736.2018.1424945](https://doi.org/10.1080/02656736.2018.1424945)

To link to this article: <https://doi.org/10.1080/02656736.2018.1424945>



© 2018 The Author(s). Published by Informa UK Limited, trading as Taylor & Francis Group



Published online: 18 Jan 2018.



Submit your article to this journal [↗](#)



Article views: 561



View Crossmark data [↗](#)

SAR thresholds for electromagnetic exposure using functional thermal dose limits

Fatemeh Adibzadeh*, Margarethus M. Paulides and Gerard C. van Rhoon

Department of Radiation Oncology, Hyperthermia Unit, Erasmus MC - Cancer Institute, Rotterdam, The Netherlands

ABSTRACT

Background and purpose: To protect against any potential adverse effects to human health from localised exposure to radio frequency (100 kHz–3 GHz) electromagnetic fields (RF EMF), international health organisations have defined basic restrictions on specific absorption rate (SAR) in tissues. These exposure restrictions incorporate safety factors which are generally conservative so that exposures that exceed the basic restrictions are not necessarily harmful. The magnitude of safety margin for various exposure scenarios is unknown. This shortcoming becomes more critical for medical applications where the safety guidelines are required to be relaxed. The purpose of this study was to quantify the magnitude of the safety factor included in the current basic restrictions for various exposure scenarios under localised exposure to RF EMF.

Materials and methods: For each exposure scenario, we used the lowest thermal dose (TD) required to induce acute local tissue damage reported in literature, calculated the corresponding TD-functional SAR limits (SAR_{TDFL}) and related these limits to the existing basic restrictions, thereby estimating the respective safety factor.

Results: The margin of safety factor in the current basic restrictions on 10 g peak spatial average SAR ($psSAR_{10g}$) for muscle is large and can reach up to 31.2.

Conclusions: Our analysis provides clear instructions for calculation of SAR_{TDFL} and consequently quantification of the incorporated safety factor in the current basic restrictions. This research can form the basis for further discussion on establishing the guidelines dedicated to a specific exposure scenario, i.e. exposure-specific SAR limits, rather than the current generic guidelines.

ARTICLE HISTORY

Received 2 October 2016

Revised 3 January 2018

Accepted 3 January 2018

KEYWORDS

Localized electromagnetic exposure; basic restrictions; safety factor; thermal dose thresholds; functional SAR limits



Introduction

To protect against any established health effect of electromagnetic (EM) exposure, international safety organizations, such as ICNIRP and IEEE, have defined basic restrictions on maximum exposure of humans to electromagnetic fields (EMF) [1,2]. Based on these guidelines at radio frequency (RF) range of EMF (100 kHz–3 GHz), exposure should not result in peak spatial average SAR ($psSAR$) that exceeds 10 W/kg as averaged over any 10 g of tissues ($psSAR_{10g}$). From here on we shall refer to this value as SAR_{BR} . This level applies to exposure of persons in occupational environments, i.e. trained adults under controlled conditions. The basis of these guidelines is to limit tissue heating below a conservative safety threshold of 1 °C.

To provide a large margin of safety, the local SAR safety threshold is lowered by a conservative safety factor. Although not quantified, it is believed that the safety factor is at least a factor of 10 and probably considerably more if the remarkable thermal tolerance in human studies is accepted as generally valid [2]. The selection of the incorporated safety factor in the current guidelines was based on informed

expert opinion rather than a rigorous quantitative process. The magnitude of safety factor for any given localised exposure scenario is unknown.

The above shortcoming becomes more critical for some applications where the safety guidelines should be relaxed to achieve better therapeutic or diagnostic results [3–5]. For instance, in medical imaging or therapy taking more risk is permissible if this provides a better diagnosis or therapeutic effect. We recently performed dose–effect relations studies and showed that exceeding the SAR_{BR} by up to at least 14 (brain [6]) and 10 (eyes [7]) times during hyperthermia (HT) cancer treatment in the head and neck region, showed no indication for any serious acute effect for any of the treated patients. In view of these publications and to align the basic SAR restrictions with the current practice, medical applications should have added flexibility in safety guidelines by taking a much smaller safety factor. This approach has been applied to some extent for magnetic resonance imaging (MRI) application in the third edition of the IEC standards [8]: safety guidelines on the maximum value for the local $psSAR_{10g}$ are doubled for the first level operation mode.

CONTACT Fatemeh Adibzadeh  f.adibzadeh@erasmusmc.nl  Hyperthermia Unit, Department of Radiation Oncology, Erasmus MC - Cancer Institute, Rotterdam, The Netherlands

*Current affiliation: Department of Electrical Engineering, Sharif University of Technology, Tehran, Iran

© 2018 The Author(s). Published by Informa UK Limited, trading as Taylor & Francis Group

This is an Open Access article distributed under the terms of the Creative Commons Attribution-NonCommercial-NoDerivatives License (<http://creativecommons.org/licenses/by-nc-nd/4.0/>), which permits non-commercial re-use, distribution, and reproduction in any medium, provided the original work is properly cited, and is not altered, transformed, or built upon in any way.

Therefore, there is a need to quantify the incorporated safety factors more precisely and to relax the limits on EM exposure accordingly.

The main objective of the current study was to quantify the incorporated safety factor in the current ICNIRP and IEEE basic restrictions for various localized RF exposure scenarios. To this end, using previously published data [9], we first translated the functional thermal dose (TD) required to induce acute local tissue damage into corresponding TD-based functional SAR limits (SAR_{TDFL}). The ratio between these SAR_{TDFL} values and SAR_{BR} is defined as safety factor. Secondly, we performed a sensitivity study to assess the changes in the calculated SAR_{TDFL} due to exposure parameters. Thirdly, we evaluated our results by comparing the SAR_{TDFL} to SAR levels in realistic clinical situations. Finally, we proposed a simple instruction to calculate SAR_{TDFL} limit for any given exposure scenario.

Methods

In the current study, we calculated the SAR_{TDFL} necessary to induce heating up to $T_{threshold}$ i.e. the corresponding steady state temperature of the lowest TD that results in tissue damage in the particular tissue type [9]. This was calculated for the centre of a spherical target within a 37°C medium (Figure 1). This target mimics a hotspot in tissue, induced by localized exposure to RF EMF.

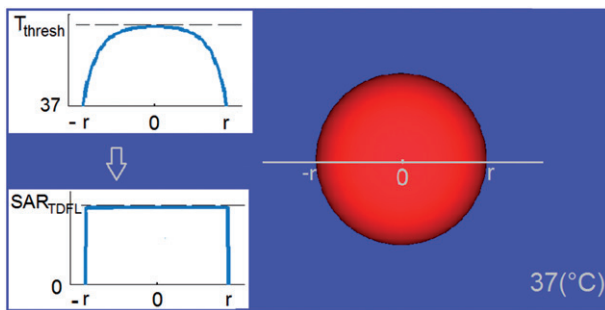


Figure 1. Main image: Modelled hotspot-mimicking a spherical target inside a tissue at 37°C . Inset images: Induction of temperatures up to $T_{threshold}$ at centre of the sphere, and the corresponding SAR_{TDFL} .

Table 1. Translation of the lowest tissue-specific CEM43 $^{\circ}\text{C}$ doses that result in thermal tissue damage in large animals (cat, dog and pig) and humans, to the corresponding temperature for exposure durations of 60, 30, 15 and 5 min. According to CEM43 $^{\circ}\text{C}$ definition (Equation (1)), the value of $T_{threshold}$ depends on the exposure duration.

Tissue	CEM43 $^{\circ}\text{C}^a$ (min)	$T_{threshold}$ ($^{\circ}\text{C}$)			
		$t = 60$ (min)	$t = 30$ (min)	$t = 15$ (min)	$t = 5$ (min)
Brain	7.5	41.5	42.0	42.5	43.6
Spinal cord	30	42.5	43.0	44.0	45.6
Peripheral nerve	45.5	42.8	43.6	44.6	46.2
Skin	288	45.3	46.3	47.3	48.8
Esophagus	120	44.0	45.0	46.0	47.6
Liver	9.9	41.7	42.2	42.7	44.0
Bladder	90.5	43.6	44.6	45.6	47.2
Prostate	30.0	42.5	43.0	44.0	45.6
Muscle	60.0	43.0	44.0	45.0	46.6
Fat	240	45.0	46.0	47.0	48.6

^aDerived from [9] and using data summarised in reviews on thermal thresholds for tissue damage [31,32].

As a first step, we translated the TD to $T_{threshold}$ for tissues used in our previous study [9] (Table 1) based on the definition of cumulative equivalent minutes at 43°C (CEM43 $^{\circ}\text{C}$). Secondly, we calculated the value of SAR_{TDFL} based on the Pennes bioheat equation (PBE) and compared its value within various tissues. Thirdly, we assessed the sensitivity of SAR_{TDFL} due to changes in the target diameter (as a result of changes in exposure frequency), exposure duration and thermal tissue properties for muscle. Muscle was selected as thermal hotspots occur most commonly in this tissue during medical applications such as HT and MRI, with a frequency range: ca. 1–1000 MHz [10] and literature values are more abundant. We calculated the SAR_{TDFL} values for target diameters of 20, 15, 10, 5, 2, 1 and 0.5 cm using various databases containing basal and thermoregulated tissue properties [11–14]. To evaluate the influence of exposure duration on the results, we compared the SAR_{TDFL} for exposure duration of 60, 30, 15 and 5 min in targets of 20, 5, 2 and 0.5 cm diameter.

Finally, we evaluated our results by comparing the calculated SAR_{TDFL} values in the current study with simulated SAR values inside a realistic anatomical model under exposure of RF EMF from head and neck HT treatment and 1.5 T MRI imaging. The simulations were performed using SEMCAD X (v.14.8.4, SPEAG, Zurich, Switzerland) and validated by matching to the experimental data [10,15].

CEM43 $^{\circ}\text{C}$ TD

Thermal dose is usually expressed in units of cumulative equivalent minutes at 43°C (CEM43 $^{\circ}\text{C}$) [16–18]. The CEM43 $^{\circ}\text{C}$ dose model expresses the thermal load on living tissues by estimating the equivalent induced thermal stress in minutes at 43°C . We translated the reported tissue-specific CEM43 $^{\circ}\text{C}$ thresholds to $T_{threshold}$ based on the CEM43 $^{\circ}\text{C}$ definition assuming a constant temperature over the duration of exposure (Table 1).

$$\text{CEM43}^{\circ}\text{C} = \sum_{i=1}^n t_i R^{(43-T)} \quad (1)$$

Where CEM43 $^{\circ}\text{C}$ is the cumulative number of equivalent minutes at 43°C , t_i is the i -th time interval, R is related to the temperature dependence of the rate of cell death ($R(T < 43^{\circ}\text{C}) = 1/4$, $R(T > 43^{\circ}\text{C}) = 1/2$) and T is the average temperature during time interval t_i .

Pennes bioheat equation

Pennes bioheat equation (PBE) [19] is often used by researchers for evaluating RF-induced temperature distributions and heating dynamics in perfused or non-perfused tissues.

$$\rho c \frac{\partial T}{\partial t} = \nabla \cdot (k \nabla T) + \rho Q + \rho SAR - \rho_b c_b \rho \omega (T - T_b) \quad (2)$$

Here, T is the tissue temperature, t is the time, SAR is the specific absorption rate, ω is the perfusion rate, ρ is the density of the medium the volume, c is the specific heat capacity, k is the thermal conductivity, Q is the metabolic heat generation rate. The subscript b denotes a blood property, respectively.

Table 2. Thermal tissue properties based on McIntosh [11], IT'IS [12], hyperplan [13], lang [14] and erasmus MC databases.

Tissue	Specific heat capacity, c (J/kg/°C)			Thermal conductivity, K (W/m/°C)			Density, ρ (kg/m ³)			Blood flow, ω (ml/min/kg)				
	Mc	IT'IS	Hyper	Mc	IT'IS	Hyper	Mc	IT'IS	Hyper	Mc	IT'IS	Hyper	Lang	Erasmus
Bladder	3514	–	3500	0.47	–	0.60	1132	–	1000	30	–	150	300	–
Brain	3653	3630	–	0.51	0.51	–	1046	1046	–	530	559	–	–	–
Eye cornea	3615	3615	–	0.50	0.54	–	1174	1051	–	0	0	–	–	–
Fat	2301	2348	3500	0.19	0.21	0.21	909	911	900	30	33	200	48	309
Kidneys	3786	3763	3500	0.54	0.53	0.58	1072	1066	1000	3960	3795	4000	4000	–
Liver	3507	3540	3500	0.51	0.52	0.64	1088	1079	1000	420	860	1000	1000	–
Muscle skeletal	3514	3421	3500	0.51	0.49	0.64	1102	1090	1000	30	37	300	180–240	457
Nerve	3452	3613	–	0.46	0.49	–	1112	1075	–	160	160	–	–	–
Skin	3310	3391	–	0.41	0.37	–	1114	1109	–	60	106	–	275 ^a	–
Spinal cord	3452	3630	–	0.46	0.51	–	1112	1075	–	160	160	–	–	–
Esophagus	–	3500	–	–	0.53	–	–	1040	–	–	190	–	–	–
Rectum	–	–	–	–	–	–	–	–	–	–	–	–	–	–
Prostate	–	3760	–	–	0.51	–	–	1045	–	–	394	–	–	–

^aDerived from [33].

In the current study, we used the Partial Differential Equations (PDE) toolbox in MATLAB (MathWorks, Natick) to solve the PBE. The calculated SAR is directly dependent on the tissue property values as inputs for PBE. The dielectric parameters were taken from the database of Gabriel [20,21]. The thermal parameters were derived from various databases as shown in Table 2.

Basal and thermoregulated tissue properties

If we compare thermal parameter values across several databases, we find small differences for density, specific heat, and thermal conductivity. For perfusion, however, differences are large because the literature values for blood perfusion are generally at resting condition (baseline temperature: 37 °C), while values at high temperatures are completely different due to thermoregulatory response of tissues under thermal stress. For local hotspots above 20 W/kg psSAR_{10g}, thermoregulated local perfusion is a major HT response mechanism [22] that largely determines RF-induced tissue temperature increase [23]. Thermoregulatory processes show typical response times on the order of 10 min [24,25]. In the current study, we did not consider the transient effect of thermoregulation, i.e. the values of parameters at steady state were always used.

Impact of local thermoregulation on RF-induced heating was analysed using databases and models of both basal and thermoregulated perfusion, as follows:

Basal perfusion

- Literature summary by McIntosh: McIntosh *et al.* standardised tissue thermal parameters by documenting 140 key papers and books and developed a database of thermal properties for around 50 human tissues [11].
- IT'IS Foundation tissue database: IT'IS foundation took an inclusive approach and incorporated all studies with varying approaches and degrees of accuracy—after eliminating studies with major flaws—to increase the parameter sample size used. This database provides the average values and information about the variability of parameters [12].

Thermoregulated perfusion

- Sigma Hyperplan tissue database: These values are provided by the HT treatment planning system HyperPlan and derived from the clinical application of deep pelvic HT with the Sigma-60 applicator. Typical values of thermal conductivity and perfusion are listed in [26], and empirically obtained values created by HT model-treatment comparison are found in [13,27].
- Temperature-dependent model by Lang: Lang *et al.* [14] employed a temperature-dependent blood perfusion model based on preclinical measurement data of [28] to improve the classical bio-heat term in PBE, which assumed a constant-rate blood perfusion within each tissue [14]. For each exposure scenario, we calculated the perfusion value based on Lang model using the corresponding T_{thresh} in Table 1.
- Erasmus MC database: We calculated the effective perfusion for tumour, muscle and fat from the measurement data obtained during deep head and neck HT treatments of nine patients that had interstitial catheters in the target region (unpublished research). The effective perfusion was reconstructed based on the thermal washout technique from temperature decay measurements [29,30].

In summary, we assume that at resting condition, the databases of McIntosh and IT'IS are more reliable because they are based on a large number of studies. Under thermal stress and other conditions that may increase perfusion, the databases/models of Erasmus MC, Hyperplan and Lang provide more reliable data as they take thermoregulated perfusion into account. In the current study, we took the Erasmus MC properties and exposure duration of 60 min (steady state exposure duration for mild HT application) as reference. For each calculation, we used the thermal parameters (specific heat capacity, thermal conductivity, density and blood perfusion) of one database. In case that a database, e.g. Lang and Erasmus MC, does not contain all parameters we took the missing parameters from the IT'IS database.

Results

T_{thresh} : steady-state temperature approximation in lieu of TD

Table 1 includes the translated T_{thresh} values from the reported tissue-specific CEM43 °C TDs based on the CEM43 °C definition (Equation (1)). It indicates that the value of T_{thresh} depends on the exposure duration, hence, the same value of TD for a specific tissue may be obtained at high temperature for a short exposure and at low temperature for a long exposure.

Functional SAR limits SAR_{TDFL} : influence of target diameter, exposure duration and tissue thermal parameters

Figure 2 shows the calculated SAR_{TDFL} for various available tissues in Table 1. The figure indicates that muscle has the lowest SAR_{TDFL} value among tissues, when applying the basal tissue property databases which are more comprehensive compared to thermoregulated databases. It also indicates that the SAR_{TDFL} increases significantly if the thermoregulated perfusion is applied. The maximum variation in calculated SAR_{TDFL} is seen in muscle, which is 10-fold greater using parameters from Erasmus MC, compared to SAR_{TDFL} estimates using the McIntosh database.

Figure 3 shows the impact of target diameter and thermal tissue parameters on the calculated SAR_{TDFL} in the muscle. It demonstrates the rapid increase in SAR_{TDFL} with decreasing target diameter, i.e. SAR_{TDFL} increases 180-fold as spherical hotspot region decreases from 20 cm to 0.5 cm diameter. The figure also indicates that the variations in the calculated SAR_{TDFL} due to the differences in thermal tissue properties among various databases are larger for bigger targets, where the tissue blood perfusion is the dominant parameter, and decreases in small targets, where thermal conduction dominates (Figure 3). The maximum variation in the calculated SAR_{TDFL} due to differences in thermal parameters over various databases is in a target of 20 cm diameter, with a 12.5-fold increase using thermoregulated perfusion (Erasmus MC database) vs. basal perfusion (McIntosh database).

Figure 4 shows the impact of exposure duration on the calculated SAR threshold. It indicates that by reduction of exposure duration, the calculated SAR_{TDFL} in targets increases, which is caused by the higher thresholds of temperature increase in tissues, i.e. according to the CEM43 °C definition, shorter exposure duration requires higher temperature for the same CEM43 °C TD (Equation (1)). This increase is more pronounced in larger targets than in small targets. For exposure duration less than

About 10 min (thermoregulatory response time) only the basal thermal tissue properties from the McIntosh database were applied. The calculated SAR limit for muscle using McIntosh database increases by 10-fold by reducing the exposure duration from 60 to 5 min in a target of 20 cm diameter. This increase is lower for smaller targets.

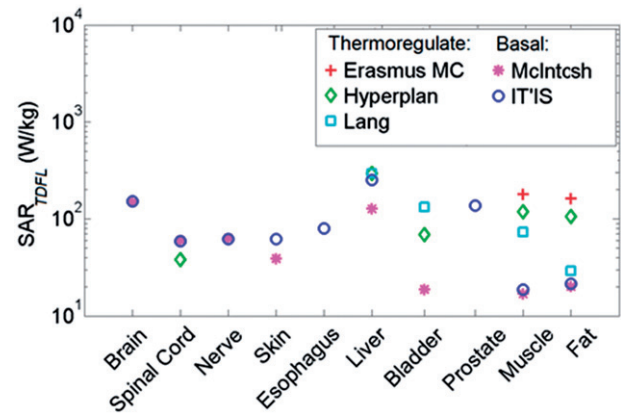


Figure 2. Comparison of SAR_{TDFL} among various tissues after 60 min exposure, using various tissue property databases. The SAR_{TDFL} values were calculated assuming that the target is uniformly heated.

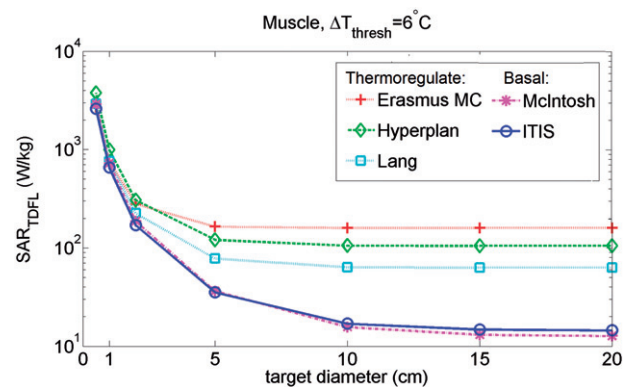


Figure 3. Impact of target diameter on the SAR_{TDFL} in muscle using various databases for thermal tissue properties. The SAR_{TDFL} values were calculated for exposure duration of 60 min.

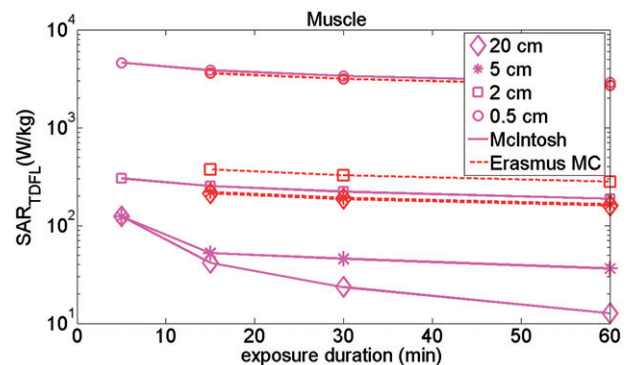


Figure 4. Impact of exposure duration on the SAR_{TDFL} after 60, 30, 15 and 5 min exposure in targets of 20, 5, 1 and 0.5 cm diameter in muscle. The results are calculated for only basal (McIntosh) and thermoregulated (Erasmus MC) perfusions, considering 10 min delay in thermoregulatory process of tissue, i.e. there is no thermoregulated perfusion for exposure duration < 10 min.

Validation of the SAR limits using clinical conditions

To validate our results, we compared the calculated SAR_{TDFL} with the SAR values that have been assessed based on complicated numerical simulation software. Hereto, we calculated and compared the SAR_{TDFL} with the simulated SAR in anatomical human models under exposure to RF EMF from HT treatment and 1.5 T MRI imaging. In our previous study we used detailed numerical EM and thermal simulations to

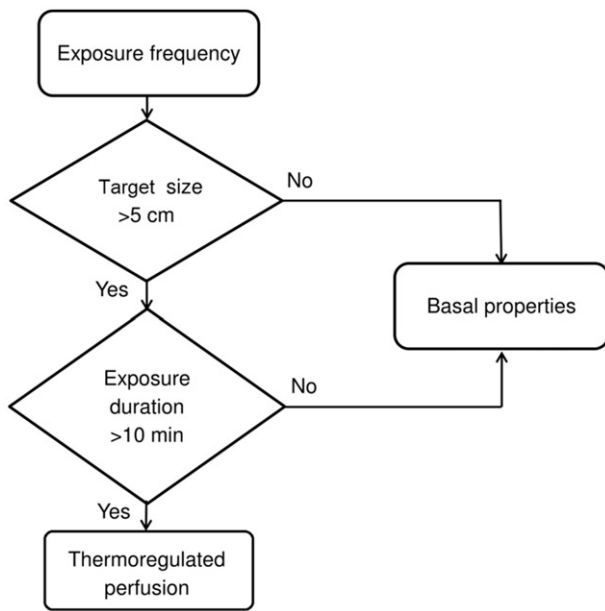


Figure 5. Instructions to calculate SAR_{TDFL} limit. The outputs are SAR_{TDFL} limits derived using basal or thermoregulated tissue properties.

assess the maximum induced SAR and temperature in patients during 60 min of HT treatment in the head and neck region [7]. The results showed that $psSAR_{10g}=191.5\text{ W/kg}$ is required to increase the temperature by 6°C in 10 g of muscle (equivalent to a spherical target of 2.6 cm diameter). The calculated SAR_{TDFL} for muscle in a target of 2.6 cm using thermoregulated Erasmus MC database is 218.3 W/kg . In addition, Murbach *et al.* [34] reported that performing MRI in the first level operating mode (OM) afforded $psSAR_{10g}$ values as large as 62 W/kg . Their results show that such $psSAR_{10g}$ value in a healthy volunteer may result in a local temperature increase of 4°C in skin tissue, using IT'IS database with temperature-dependent perfusion. Our calculation shows that a SAR_{TDFL} of 83 W/kg is required to induce 4°C at the centre of 2.8 cm spherical target (equivalent to 10 g of skin) using the same tissue properties. The uncertainty of SAR_{TDFL} from simulations was 23% in HT [7] and 42% in MRI [34] studies. Therefore, the differences between the calculated vs. simulated SAR values are less than the uncertainty of numerical modelling (HT: 12% vs. 23% and MRI: 33% vs. 42%).

Guidelines to calculate SAR_{TDFL}

Finally, we provide a decision making flowchart that demonstrates instructions to calculate the SAR_{TDFL} limit (Figure 5). Hereto we first need to determine the size of target in a specific tissue which is estimated by the RF wavelength in a lossy dielectric or tissue [35]. For hotspots with diameter larger than 5 cm, the blood perfusion is the most influential parameter. Therefore, thermal tissue properties under thermal stress (e.g. ErasmusMC, Hyperplan and Lang databases) should be used to calculate SAR_{TDFL} when the exposure duration is longer than 10 min, and the thermoregulatory response of tissue is activated [24,25]. This excludes hotspots with a diameter less than 5 cm, since for small hotspots thermal conductivity is the determinant parameter that has

similar values amongst the property databases. If the exposure duration is shorter than 10 min, we propose to use the databases for basal/resting conditions (e.g. McIntosh and IT'IS).

Discussion

The defined current limits for maximum human exposure to RF EMF are conservative and incorporate large safety factors. The limits are overly restrictive for some EMF based medical applications such as HT and MRI in which increasing the limits provides a better diagnosis or therapeutic effect. Increasing the limits requires quantification of the incorporated safety factors which were originally selected based on expert opinion rather than a rigorous quantitative process. The main objective of the current study was to quantify the incorporated safety factor in the current basic restrictions for various local exposure scenarios. This was achieved by calculating the SAR_{TDFL} limits based on the lowest TDs that result in local acute tissue damage, derived from our previous study [9]. The calculated SAR_{TDFL} was analysed for various target sizes, exposure durations and databases of thermal tissue properties. Our results uncover the large safety factors for muscle tissue between the SAR levels at which functional changes occur (SAR_{TDFL}) and the current basic SAR restrictions (SAR_{BR}) (Table 3). The magnitude of the safety factor ranged from 10.9 to 31.2 for $psSAR_{10g}$. The lower and upper bounds of the range were obtained for exposure durations of 60 and 10 min (10 min = typical delay of the thermoregulatory process) using thermoregulated perfusion from the Erasmus MC database, i.e. the reference database in this study. Table 3 also shows the ratio between SAR_{TDFL} and MRI guidelines (as an important guideline for an EMF-based medical application).

The presented approach in the current study can be extended to any tissue for which thermal threshold data is available. Amongst the tissues studied (Table 1), we selected muscle for three reasons, the common occurrence of thermal hotspots upon medical applications of RF EMF, availability of a wealth of data, and calculated SAR_{TDFL} limit being the lowest among studied tissues (Figure 2).

The quoted results can be regarded as conservative estimates since we employed the minimum value of the reported CEM43 $^\circ\text{C}$ doses amongst all available data for humans and animal species. For instance, the lowest CEM43 $^\circ\text{C}$ dose for thermal damage in muscle has been reported as 160 min in dogs and 60 min in pigs [36,37]. The safety factor in Table 3 is calculated using the lower of these values. In addition, functional changes in humans occur at higher TDs due to much more efficient thermoregulatory system in humans compared to animals [2]. Therefore, while additional research on TDs in humans will be invaluable, we believe that the incorporated safety factor for humans is larger than the values shown in Table 3.

We also assessed the sensitivity of the calculated SAR_{TDFL} to exposure parameters, i.e. the size of hotspot, exposure duration and thermal tissue properties. Our results show that the size of heated volume has a major impact on the SAR_{TDFL} , i.e. the calculated SAR_{TDFL} increases rapidly with

Table 3. Safety factor between functional localised SAR limits (SAR_{TDFL}) in muscle and the basic restrictions on $psSAR_{10g}^a$ (SAR_{BR}) in the common generic guidelines [1,2] and also the restrictions on $psSAR_{10g}^a$ in the MRI guideline (SAR_{MR}) [8]. The lower and upper bounds of the range of safety factor were obtained for exposure durations of 60 and 10 min. The safety factor is valid over the same RF range that the basic restrictions are defined (100 kHz–3 GHz).

	SAR_{BR} (W/kg): persons in controlled environments (ICNIRP, IEEE)	SAR_{MR} (W/kg): first level controlled operation mode (MRI guideline)	SAR_{TDFL} (W/kg): (current study)	Safety factor	
				(SAR_{TDFL}/SAR_{BR})	(SAR_{TDFL}/SAR_{MR})
Head and trunk	10	20	218.4–312.3 ^b	21.8–31.2	10.9–15.6
Extremities and ear pinnae ^c	20	40	218.4–312.3 ^b	10.9–15.6	5.4–7.8

^aPeak spatial SAR averaged over any 10 g of tissue.

^bCalculated in a target (in shape of sphere) of 2.6 cm diameter, equivalent to 10 g of muscle.

^cThe extremities are the arms and legs distal from the elbows and knees, respectively.

decreasing target diameter. The reason for this is the increasing surface-to-volume ratio with decreasing target diameter which leads to a stronger dissipation of the generated heat into surrounding tissue. In turn this leads to a higher required SAR for inducing heating inside the target. This finding is in line with the higher delivered SAR level of deep HT treatment in the head and neck region (*ca.* 75 W/kg) compared to pelvic region (*ca.* 16 W/kg) which is mainly due to smaller size of target in the head and neck region [38,39]. This finding also confirms the relationship between the SAR and tumour size in magnetic nanoparticle HT reported previously [40]. Regarding the sensitivity of results to exposure duration, we found that reduction of exposure duration results in higher thresholds of safe temperature-increase and consequently to a maximum of 10-fold increase in SAR_{TDFL} (Figure 4). Finally, to assess sensitivity of the results to the tissue properties, we used various available tissue property databases. The results show that the impact of (delayed) temperature-regulated perfusion on the SAR_{TDFL} is the most influential tissue parameter. Therefore, more research on local thermoregulatory and tissue damage processes is of high importance. In a target of 20 cm in muscle, thermoregulated perfusion increases SAR_{TDFL} by up to 12.5-fold, compared to basal perfusion at resting condition. In smaller heating volumes, where the surface-to-volume ratio is big, perfusive effects are almost non-existent, and thus thermal conductivity becomes the primary mechanism of heat transport (Figure 3).

To validate our results, we compared the SAR limits for two types of tissue (muscle and skin) as calculated in the current study (SAR_{TDFL}) vs. the equivalent simulated value ($psSAR_{10g}$) from numerical calculations and experimental investigations in HT and MRI applications. The comparison shows that the calculated results in the current study are consistent with the simulations and therefore, the SAR_{TDFL} limits are valid.

Lastly, we should mention that the current study had a number of assumptions. First, we assumed a constant temperature over 60 min of treatment. This is a conservative approach (worst case) as heating is not expected to be either spatially or temporally constant during the entire HT session. In case of shorter exposure duration, the temperature and also the calculated SAR will be higher according to the CEM43 °C definition (Equation (1)). Second, for comparison of SAR_{TDFL} among various tissues (Figure 2), we calculated SAR_{TDFL} assuming that the target is uniformly heated. By this

simplification, the conduction term in PBE can be set to zero and hence the PBE can be solved analytically. Third, no other temperature related effects were considered, e.g. change of SAR distribution due to thermoregulation dependent dielectric parameter. Last, in this study, the perfusion is the microscopic perfusion and the effect of macroscopic perfusion is neglected, making our approach even more conservative near major vessels.

Conclusions

The basis for the current basic restrictions, defined by ICNIRP and IEEE, is to keep local tissue temperature rise under 1 °C for 30 min of EMF exposure. However, thermal tissue damage occurs at much higher TDs. In the current study, we explored the actual safety margin that current guidelines provide in preventing thermal tissue damage in various localised exposure scenarios. Based on the available TD-effect data in literature, we calculated functional SAR limits (SAR_{TDFL}) and consequently quantified the safety factor between SAR_{TDFL} and the current basic restrictions (SAR_{BR}). We found that the safety factor for the most common hotspot location, *i.e.* muscle, is large: depending on the exposure duration 10.9–31.2. We concluded that the current basic restrictions appear to be conservative and that functional limits and application-specific modelling provide a valuable tool for tailoring the guidelines in specific applications.

The benefit of changing from generic to application-specific restrictions is that it facilitates a much better balance between the need for the exposure, e.g. diagnostic or therapeutic, and the risk from thermal damage. Such an approach might be beneficial for patients undergoing MRI to detect abnormalities in anatomy, where higher quality imaging that can yield better diagnoses would exceed current SAR safety limits. Also in HT treatments, the functional limits may have potential for balancing the probability of thermal toxicity against probability of tumour control.

Disclosure statement

No potential conflict of interest was reported by the authors.

Funding

This work was supported by ZonMw (85800002).

References

- [1] ICNIRP (1998). Guidelines for limiting exposure to time-varying electric, magnetic, and electromagnetic fields (up to 300 GHz). *Health Phys* 74:494–522.
- [2] IEEE (2005). Standard for safety levels with respect to human exposure to radio frequency electromagnetic fields, 3 kHz to 300 GHz, Std C95.1.
- [3] Crezee H, van Leeuwen CM, Oei AL, *et al.* (2016). Thermoradiotherapy planning: integration in routine clinical practice. *Int J Hyperthermia* 32:41–9.
- [4] Winter L, Oberacker E, Paul K, *et al.* (2016). Magnetic resonance thermometry: methodology, pitfalls and practical solutions. *Int J Hyperthermia* 32:63–75.
- [5] Balidemaj E, Kok HP, Schooneveldt G, *et al.* (2016). Hyperthermia treatment planning for cervical cancer patients based on electrical conductivity tissue properties acquired in vivo with ept at 3 t mri. *Int J Hyperthermia* 32:558–68.
- [6] Adibzadeh F, Verhaart RF, Verduijn GM, *et al.* (2015). Association of acute adverse effects with high local SAR induced in the brain from prolonged RF head and neck hyperthermia. *Phys Med Biol* 60:995–1006.
- [7] Adibzadeh F, van Rhooen GC, Verduijn GM, *et al.* (2016). Absence of acute ocular damage in humans after prolonged exposure to intense RF EMF. *Phys Med Biol* 61:488–504.
- [8] International Electrotechnical Commission. IEC. International standard, Medical equipment IEC 60601-2-33: particular requirements for the safety of Magnetic resonance equipment, 3rd edition; Geneva: IEC, 2010.
- [9] van Rhooen GC, Samaras T, Yarmolenko PS, *et al.* (2013). CEM43 °C thermal dose thresholds: a potential guide for magnetic resonance radiofrequency exposure levels? *Eur Radiol* 23:2215–27.
- [10] Murbach M, Neufeld E, Capstick M, *et al.* (2014). Thermal tissue damage model analyzed for different whole-body SAR and scan durations for standard MR body coils. *Magn Reson Med* 71:421–31.
- [11] McIntosh RL, Anderson V. (2010). Comprehensive tissue properties database provided for the thermal assessment of a human at rest. *Biophys Rev Lett* 5:129–51.
- [12] Hasgall PA, Neufeld E, Gosselin MC, *et al.* IT'IS Database for thermal and electromagnetic parameters of biological tissues. www.itis.ethz.ch/database, 2015. Version 3.0.
- [13] Sreenivasa G, Gellermann J, Rau B, *et al.* (2003). Clinical use of the hyperthermia treatment planning system HyperPlan to predict effectiveness and toxicity. *Int J Radiat Oncol Biol Phys* 55:407–19.
- [14] Lang J, Erdmann B, Seebass M. (1999). Impact of nonlinear heat transfer on temperature control in regional hyperthermia. *IEEE Trans Biomed Eng* 46:1129–38.
- [15] Paulides MM, Bakker JF, van Rhooen GC. (2007). Electromagnetic head-and-neck hyperthermia applicator: experimental phantom verification and FDTD model. *Int. J. Radiat Oncol Biol Phys* 68:612–20.
- [16] Sapareto SA, Dewey WC. (1984). Thermal dose determination in cancer therapy. *Int J Radiat Oncol Biol Phys* 10:787–800.
- [17] Dewhurst MW, Vujaskovic Z, Jones E, Thrall D. (2005). Re-setting the biologic rationale for thermal therapy. *Int J Hyperthermia* 21:779–90.
- [18] van Rhooen GC. (2016). Is CEM43 still a relevant thermal dose parameter for hyperthermia treatment monitoring? *Int J Hyperthermia* 32:50–62.
- [19] Pennes HH. (1948). Analysis of tissue and arterial blood temperatures in the resting human forearm. *J Appl Physiol* 1:93–122.
- [20] Gabriel S, Lau RW, Gabriel C. (1996). The dielectric properties of biological tissues: II. Measurements in the frequency range 10 Hz to 20 GHz. *Phys Med Biol* 41:2251–69.
- [21] Gabriel S, Lau RW, Gabriel C. (1996). The dielectric properties of biological tissues: III. Parametric models for the dielectric spectrum of tissues. *Phys Med Biol* 41:2271–93.
- [22] Stolwijk JAJ. (1980). Mathematical models of thermal regulation. *Ann N Y Acad Sci* 335:98–106.
- [23] Laakso I, Hirata A. (2011). Dominant factors affecting temperature rise in simulations of human thermoregulation during RF exposure. *Phys Med Biol* 56:7449–71.
- [24] Chou CK, Guy AW. (1983) Electromagnetic heating for therapy. Technical report, University of Washington.
- [25] Gouit C, Madon E, Allegro D, *et al.* (1998). Perfusion and thermal field during hyperthermia. Experimental measurements and modelling in recurrent breast cancer. *Phys Med Biol* 43:2831–43.
- [26] Wust P, Stahl H, Loffel J, *et al.* (1995). Clinical, physiological and anatomical determinants for radiofrequency hyperthermia. *Int J Hyperthermia* 11:151–67.
- [27] Wust P, Seebass M, Nadobny J, *et al.* (1996). Simulation studies promote technological development of radiofrequency phased array hyperthermia. *Int J Hyperthermia* 12:477–94.
- [28] Song CHW, Lokshina A, Rhee JG, *et al.* (1984). Implication of blood flow in hyperthermia treatment of tumours. *IEEE Trans Biomed Eng* 31:9–16.
- [29] Roemer R, Fletcher A, Cetas T. (1985). Obtaining local SAR and blood perfusion data from temperature measurements: steady state and transient techniques compared. *Int J Radiat Oncol Biol Phys* 11:1539–50.
- [30] Waterman F, Tupchong L. (1991). Blood flow in human tumors during local hyperthermia. *Int J Radiat Oncol Biol Phys* 20:1255–62.
- [31] Dewhurst MW, Viglianti BL, Lora-Michiels M, *et al.* (2003). Basic principles of thermal dosimetry and thermal thresholds for tissue damage from hyperthermia. *Int J Hyperthermia* 19:267–94.
- [32] Yarmolenko PS, Moon EJ, Landon C, *et al.* (2011). Thresholds for thermal damage to normal tissues: an update. *Int J Hyperthermia* 26:1–26.
- [33] Drizdal T, Togni P, Visek L, Vrba J. (2010). Comparison of constant and temperature dependent blood perfusion in temperature prediction for superficial hyperthermia. *Radioengineering* 19:281–9.
- [34] Murbach M, Neufeld E, Kainz W, *et al.* (2013). Whole-Body and Local RF absorption in human models as a function of anatomy and position within 1.5T MR body coil. *Magn Reson Med* 71:839–45.
- [35] Winter L, Oezerdem C, Hoffmann W, *et al.* (2015). Thermal magnetic resonance: physics considerations and electromagnetic field simulations up to 23.5 Tesla (1GHz). *Radiation Oncology* 10:201.
- [36] Rabkin BA, Zderic V, Crum LA, *et al.* (2006). Biological and physical mechanisms of HIFU-induced hyperecho in ultrasound images. *Ultrasound Med Biol* 32:1721–9.
- [37] Nosaka K, Muthalib M, Lavender A, Laursen PB. (2007). Attenuation of muscle damage by preconditioning with muscle hyperthermia 1-day prior to eccentric exercise. *Eur J Appl Physiol* 99:183–92.
- [38] Paulides MM, Verduijn G, Van Holthe N. (2016). Status quo and directions in deep head and neck hyperthermia. *Radiat Oncol* 11:21
- [39] Adibzadeh F, Bakker JF, Paulides MM, *et al.* (2015). Impact of head morphology on local brain specific absorption rate from exposure to mobile phone radiation. *Bioelectromagnetics* 36:66–76.
- [40] Dutz S, Hergt R. (2013). Magnetic nanoparticle heating and heat transfer on a microscale: basic principles, realities and physical limitations of hyperthermia for tumour therapy. *Int J Hyperthermia* 29:790–800.